International Journal of Engineering

Experimental Investigation and Thermodynamic Modeling of Zn^{+2} and Ni^{+2} Extraction from Zn Plant Residue using D2EHPA

M. Mohammadzadeh*, H. Bagheri, S. Ghader*

Department of Chemical Engineering, Faculty of Engineering, Shahid Bahonar University of Kerman, Kerman, Iran

P A P E R   I N F O

A B S T R A C T

Zinc plant filter cake contains valuable metals that can be reused as a source for obtaining these metals. This study describes an experimental two stage study on the extraction of zinc and nickel from waste zinc filter cake which includes acid leaching of zinc filter cake followed by organic phase aided extraction of metals from the leaching solution. To determine the optimum leaching condition a comprehensive study of the recovery of chemical elements from spent plant residues was experimentally studied at different levels of acid concentrations at different temperatures while measuring chemical elements concentration with respect to time. Experimental results showed that 99% recovery of Ni^{2+}, Zn^{2+} and 89% recovery of Pb^{2+} can be achieved at following optimum conditions: 2M nitric acid, T= 358.15 K after 1.5 h of acid leaching at S/L=1/10. Then, the extraction of Zn^{2+}, Ni^{2+}, and Pb^{2+} was carried out by di-(2-ethylhexyl) phosphoric acid (D2EHPA) that was diluted with kerosene in equal phase ratio and the effect of extractant concentration and pH was studied at T = 298.15 K. Results showed that an increase in pH and extractant concentration can greatly increase zinc and nickel extraction to a maximum achievable amount of 95% and 90 % for Zn^{2+} and Ni^{2+}, respectively by 25 (v/v%) D2EHPA at pH = 5.5 and organic to aqueous phase ratio (O/A) = 1/1. For modeling of equilibrium concentrations in organic and aqueous phases and activity coefficients calculation, Electrolyte-UNIQUAC-NRF, UNIQUAC-NRF, NRTL and NRTL-based local composition models were used. After that, adjusted parameters were successfully used for calculation of the equilibrium constant of the unknown parameters and the extraction reaction. The obtained results of thermodynamic modeling were in well agreement with the experimental data.

doi: 10.5829/ije.2023.36.11b.07

1. INTRODUCTION

In recent years, because of increasing the consumption of metals along with the simultaneous depletion of primary resources, more attention has been drawn to the recovery of metals from secondary resources, including waste residues from zinc plants. Recovering the valuable content of these resources can have both economic and ecological advantages. Some industrial wastes are classified as the main resources of different metals [1, 2]. Metals or minerals production from ores through pyro/hydro-metallurgical processes usually causes enormous amount of residues [3, 4]. For example, zinc industrial residue, which is produced in zinc ores processing contains some valuable metals, e.g., Ni, Pb as well as Zn that can be beneficially recovered for further processing. Thus, recovering these metals from the secondary resources as well as natural minerals for the high value products, is necessary and important for effective use of these resources [5]. Nowadays, several techniques such as electrolysis, cementation, liquid-liquid extraction, precipitation, and ion exchange have been applied to separate and recover metals from zinc plant residue [6, 7]. The hydrometallurgical route is one of the most widely used approaches for recovering valuable metals from zinc plant residue which mainly involves leaching with an acid solution followed by the extraction of metal ions

Corresponding Authors Emails:
masumeh70mohammadzadeh@gmail.com (M. Mohammadzadeh),
sattarghader@gmail.com (S. Ghader)

from leaching solution [8]. Solvent extraction, as an efficient separation and purification technology, can achieve the selective extraction of target elements and has been widely used in metal hydrometallurgy, heavy metal wastewater treatment, and other fields [8, 9].

Solvent extraction process of Ni, Zn, and Pb from aqueous solution by several commercial extractants have been studied by researchers. They were trying to understand the role and effect of influencing parameters like pH of solution and type and concentration of extractant [10, 11]. For example, acidic extractants (Cyanex 302 [12], D2EHPA [13], and Cyanex 272 [14]) and chelating extractants (LIX 984N [15], LIX 63 [16], and LIX 84 [17]) have been used for this purpose. Di-2-ethyl hexyl phosphoric acid (D2EHPA) as a classical extractant, has been widely used in extraction and separation of the divalent transition metals such as zinc, manganese, nickel, cobalt and copper [18-20]. According to the previous researches, for enhanced separation of Zn from acid solution by D2EHPA, another extractant along with D2EHPA must be used [21, 22]. For instance, Hosseini et al. [23] found the desired extraction of manganese and zinc was obtained using a mixture of Cya-nex 302 and D2EHPA. Alike results were presented by Babakhani et al. [24] for separation of Ni^{2+} and Cd^{2+}. Another report by Innocenzi and Veglio [25], revealed combination D2EHPA and Cya-nex 272 was more effective for separation of Mn^{2+} and Zn^{2+} than Cya-nex 272.

Mathematical modeling is a key step in a solvent extraction process and it is necessary for designing, controlling and optimization of the process [26-29]. Thus, an appropriate model is necessary for prediction a solute distribution coefficient and thermodynamic equilibrium constant of the extraction reaction [30]. Electrolyte solutions are very important in several chemical industries and biological processes. Since they are known non-ideal solutions even at low concentrations, or in some processes like gas sweetening, which electrolyte solutions have high concentration, accurate thermodynamic models are needed. Therefore, modeling and predicting the thermodynamic properties of electrolyte solutions is of great importance to predict an accurate model for a wide range of concentrations [31-40]. Some models such as Bromley model, Scatchard-Hildebrand model, Pitzer virial expansion equations and Guggenheim quasi-lattice model have been used for activity coefficient (γ_i) calculation of electrolyte and non-electrolyte solutions [37-50]. Although in the mentioned studies, γ_i was not calculated, or the non-ideality of a phase was ignored due to the complexity of the liquid-liquid extraction process, several of these models might not be accurate enough to correlate the activity coefficients of high concentration of aqueous electrolyte solutions. Some significant researches have been carried

out by Thomsen et al. [45], Pitzer [41, 42], Cruz and Renon [43], Zhao et al. [44], Chen et al. [46], Haghtalab and Vera [47] and Sadeghi [48] that the excess Gibbs energy functions based on the concept of local composition has been developed and are among the most successful electrolyte models. Haghtalab and Peyvandi [51] developed Electrolyte-UNIQUAC-NRF model for description the behavior of binary electrolyte and multi-component solution in a concentration range and at high temperature. This model is based on local-composition approach. Furthermore, Chen et al. [49] extended the e-NRTL model for single electrolyte solution and single solvent systems. Chen et al. [49] used Pitzer-Debye-Hückel equation [50] and local composition model based on NRTL for characterization of long and short range interactions, respectively.

In this work, we planned to examine the extraction of Zn^{2+}, Ni^{2+}, and Pb^{2+} from zinc plant filter cake (ZPFC) combined with various metal ions. First, the influences of different processes factors on the extraction of metal ions were experimentally calculated. Next, the equilibrium extraction of Ni^{2+} and Zn^{2+} ions from HNO_3 solution were model based on a thermodynamic model. Hence the Electrolyte-UNIQUAC-NRF and UNIQUAC-NRF equations were used for γ_i calculation for aqueous solution and organic phase, respectively. Finally, the result of both equations were compared with NRTL and a new NRTL-based local composition models.

2. EXPERIMENT METHOD

2. 1. Chemicals and Equipment   The ZPFC employed in the experiments was supplied from the zinc manufacturing plant in Zanjan (Iran) and was determined by the X-ray fluorescence (XRF) technique (ARL ADVANTX+, Switzerland). Nitric acid (purity of 65%) and the organic extractant, D2EHPA (purity of 97%) were prepared from Merck and kerosene was purchased from Esfahan Oil Refinery Co. (purity of 97%). Sodium hydroxide pellets (purity of 99%, Merck) were used to adjust pH values. The aqueous and organic phases were mixed using a mechanical stirrer. The operating temperature and pH values were monitored using a thermometer and pH meter, respectively. Moreover, metal ions concentrations in the aqueous and organic solutions were analyzed by AAS (Absorption Spectrophotometer) and mass balance, respectively.

2. 2. Experimental Procedure   The experimental procedure that was used in this communication is illustrated in Figure 1. The method included two main operating units: 1. leaching process of zinc filter cake and 2. solvent extraction process; the leach solution of step 1 is utilized for the separation, according to step 1,

an aqueous phase was supplied by dissolving of appropriate values of zinc filter cake and HNO_3 in distilled water. During the leaching process, the influence of acid concentration, time and operating temperature were investigated. In all experiments, 30 g of zinc plant filter cake (ZPFC) was mixed with 300 mL of HNO_3 (0.25-2 M), S/L=1/10, and after that stirred in the bottom three-necked flask at a speed equal to 600 rpm with a mechanical stirrer. The leaching process of all elements was investigated at time range of 30-120 min and temperature in the range of 298.15-358.15 K. The concentration of each ion in the leaching solution was obtained by absorption spectrophotometer and in the second step, in all solvent extraction tests, O/A=1/1. After that, 25 mL of each phase was blended on the mechanical stirrer and the pH value was continuously controlled during the experiment. Nitric acid (2 M) and sodium hydroxide (4 M) were applied to modify the pH. The organic and aqueous phases were separated at desired pH value by a separation funnel and after 10 min the equilibrium achieved. Then, the aqueous phase was sampled for analysis of the extracted ions. The percentage of extraction of metal ions were calculated using Equation (1) and the distribution ratio Zn^{2+} and Ni^{2+} from other metal ions. The ZPFC was oven-dried for 24 h at 303.15 K and then milled into particles of less than 0.1 mm for further analysis. The XRF analysis of the ZPFC presented in Figure 2. The percentage of extraction

was determined by using Equation (2):

$$Extraction\ (\%) = \frac{C_i - C_{aq}}{C_i} \times 100 \tag{1}$$

$$D = \frac{[C]_{org}}{[C]_{aq}} \tag{2}$$

where, C_i is the initial metal ions concentration in the aqueous phase and C_{aq} is the metal ions concentration in the aqueous phase after extraction and C_{org} is the metal ions concentration in the organic phase after extraction.
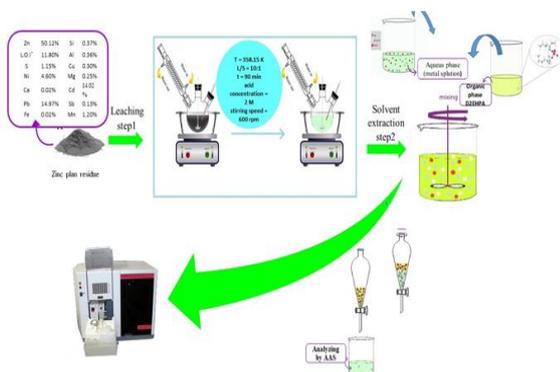
Figure1. The schematic of the experimental process
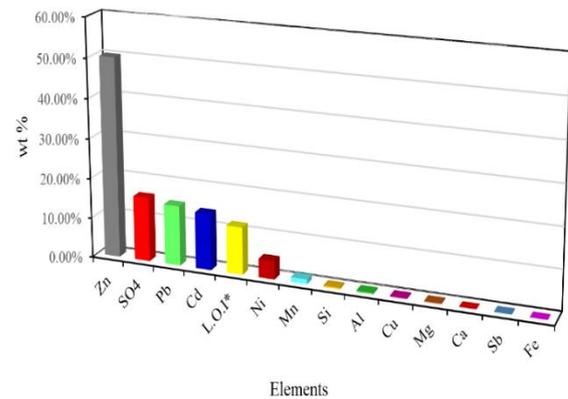
Figure 2. The chemical composition of the ZPFC using XRF analysis
*loss on ignition – the filter cake weight reduction after being ignited

3. RESULTS AND DISCUSSION

3. 1. Leaching

3. 1. 1. Result of Acid Concentration
The influence of some important factors, containing temperature, operation time and acid concentration are studied on the leaching process. ZPFC is leached with nitric acid solution followed by dissolution and solvent extraction of objective ions from the leached solutions [52]. Nevertheless, hydrometallurgical behavior creates a vast acidic wastes value that if disposed in environment reasons dangerous health problems and ecological imbalance. Among a huge number of acids, HNO_3 is most accomplished leaching agent as high oxidation potential of HNO_3 and less non-soluble residue evolution. Despite high value of HNO_3, it can be recovered again with hydrometallurgical behavior. HNO_3 can be easily recycled via external NO_x oxidation [53-56]. Generally, concentration of acid has pronounced influence on the extraction of metal and it is one of the main factors to be investigated for optimization condition for dissolution of metal ions, range of which was studied with conducting a number of experiments at various acid concentration using ZPFC. Figure 3(a) illustrates dissolution of metal ions from ZPFC by changing HNO_3 concentration in the range of 0.25-2 M,1:10 L/S, temperature (358.15 K) and contact time (1.5 h). Ni^{2+} (100%) and Zn^{2+} (99%) ions were recovered in 2 M HNO_3. But for 0.25 M HNO_3 the extraction of Ni^{2+} (33%) and Zn^{2+} (23%) was low. Also, Pb^{2+} ion was quite leached from the ZPFC (almost 89%).

3. 1. 2. Result of Temperature and Time
Figure 3 (b-d) illustrates the influence of both time reaction and operating temperature on dissolution of metal ions with 2 M HNO_3. As can be seen, both temperature and
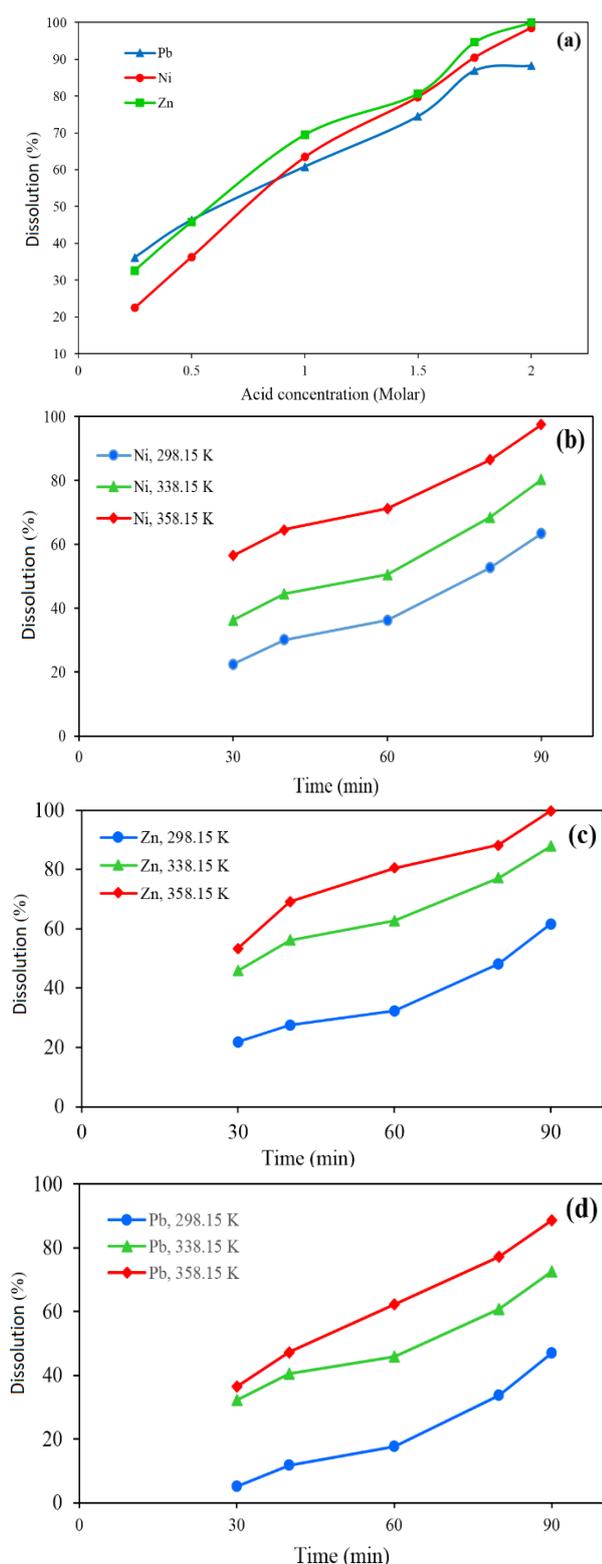
Figure 3. Factors affecting metal ions dissolution from ZPFC, S/L=1/10, (a) Influence of amount of acid on Zn^{2+}, Ni^{2+}, and Pb^{2+} dissolution at T = 358.15 K, and t = 1.5 h, Effect of temperature and time on (b) Ni^{2+}, (c) Zn^{2+}, and (d) Pb^{2+} dissolution in concentration of 2 M acid, S/L=1/10, speed of agitation: 600 rpm

reaction time had a significant influence on Zn^{2+}, Ni^{2+}, and Pb^{2+} leaching. For instance, at 298.15 K only 22.5% Ni^{2+} and 21.8% Zn^{2+} was recovered and recovery was finalized at 358.15 K.

3. 2. Solvent Extraction After investigating leaching process, the extraction of Zn^{2+}, Ni^{2+}, and Pb^{2+} were studied. All experimental tests were performed at the pH range 2-6, O/A=1/1, and T = 298.15 K. Referring to Figure 4(a), complete extraction of Ni^{2+} and Zn^{2+} ions, was occurred at higher value of pH. According to Equation (4) di-(2-ethylhexyl) phosphoric acid release hydrogen ion (H$^+$) during extraction process. Thus, increasing pH leads to increase extraction of metal from aqueous media. The extraction of Ni^{2+} and Zn^{2+} is remarkably being depending on an acidic extractant like D2EHPA and pH. There is significant difference in the treatment of each metal. The roughly a half of Zn^{2+} and almost all of Ni^{2+} ions were extracted by D2EHPA whereas Pb^{2+} remained in the aqueous solution. Furthermore, the percentage of the extraction of Pb^{2+} was 12.8 % and the pH variations had negligible effect on it.

The influence of concentration of D2EHPA on the Zn^{2+}, Ni^{2+} and Pb^{2+} extraction using 2-25 percent volume/volume of D2EHPA in kerosene at pH = 5.5, and T = 298.15 K was studied. Referring to Figure 4(b), increasing D2EHPA concentration have no remarkable effect on Pb^{2+} extraction, while the extraction percentage of Zn^{2+} and Ni^{2+} had different behavior. The obtained experimental results showed rising in D2EHPA concentration leads to remarkable extraction of Ni^{2+} (95.5%) and Zn^{2+} (96.1%). Consequently, the high values of D2EHPA concentration had effective influence on Zn^{2+} and Ni^{2+} extraction.

Aghazadeh et al. [56] studied zinc extraction from synthetic sulfate solution using D2EHPA diluted with kerosene. In their study tributyl-phosphate (TBP) showed positive synergism at concentration of 5% (v/v) and negative synergism effect at concentrations of 2% and 10%. Zinc extraction efficiency increased from 90 to 98% for experiments with 5%, 15%, and 20% D2EHPA concentrations when TBP concentration was 5%. However, their study was limited to zinc extraction from synthetic sulfate solution. Aghdam et al. [57] also, studied the possibility of separation of Zn^{2+} and Cd^{2+} metal ions from chloride solutions by (D2EHPA) in kerosene as a diluent. In fact, the aqueous phase was obtained by brine leaching of zinc leaching filter cakes. They concluded D2EHPA is capable of extracting and separating zinc from cadmium in chloride solutions at pH = 3 with approximately 99% yield a negligible co-extraction of cadmium.

3. 3. Thermodynamic Modeling The γ_i in organic and aqueous phases are needed for calculation
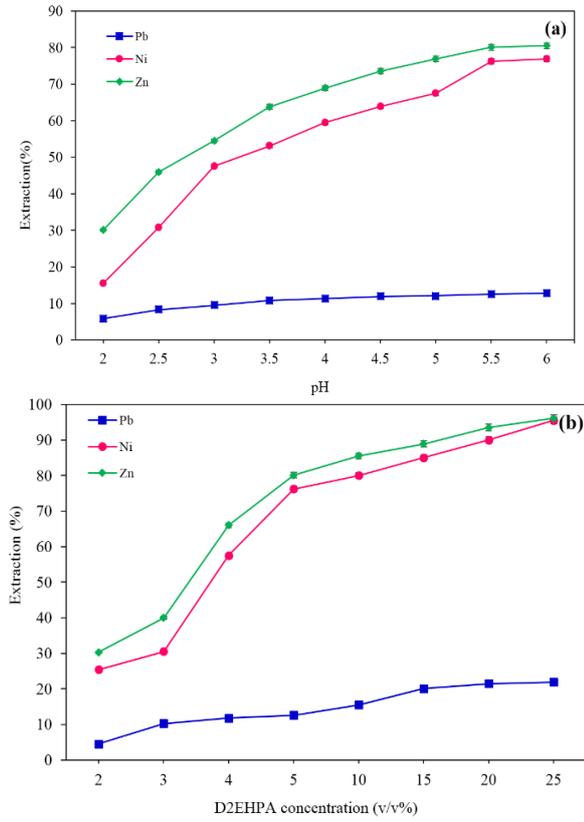
Figure 4. Factors affecting Zn^{2+}, Ni^{2+}, and Pb^{2+} extraction from ZPFC, 2 M HNO_3 solution ($[Zn^{2+}]$ = 49.51 g/L, $[Ni^{2+}]$ = 4.42 g/L and $[Pb^{2+}]$ = 14.06 g/L), (a) Effect of pH on Zn^{2+}, Ni^{2+}, and Pb^{2+} extraction at T = 298.15 K, 5 percent v/v solution of D2EHPA in kerosene, and O/A=1/1, (b) Effect of concentration of D2EHPA in kerosene on Zn^{2+}, Ni^{2+}, and Pb^{2+} ions extraction at pH = 5.5, T = 298.15 K, and O/A=1/1

K_{ex} parameter (equilibrium constant), which can be utilized to predict the concentration equilibrium of ion in the organic phase. In this study, Electrolyte-UNIQUAC-NRF (for aqueous phase) and UNIQUAC-NRF (for organic phase) models were used for γ_i calculation. These models also were compared with NRTL and a new NRTL-based local composition model [58-66]. The more details of used models are given in Appendix A. The Genetic Algorithm (GA) was used to calculate the factors of the models and K_{ex} by a regression analysis of the extraction equilibrium data. The objective function (*OF*) for GA is as following (Equation (3)):

$$OF = \frac{100}{N}\left(\Sigma \left| \frac{\overline{[Zn]}^{Cal.} - \overline{[Zn]}^{exp.}}{\overline{[Zn]}^{exp}} \right| + \left| \frac{\overline{[Ni]}^{Cal.} - \overline{[Ni]}^{exp.}}{\overline{[Ni]}^{exp}} \right| \right) \quad (3)$$

The superscripts "*cal*"of and "*exp*" are the calculated and the experimental values, respectively and *N* is the number of experimental points. The thermodynamic modeling will be performed based on following algorithm:

Algorithm 1: Proposed method

1: Input Initial concentration and experimental equilibria date for pH and $[Ni^{2+}]$ and $[Zn^{2+}]$

2: Initial assumption for parameters of models and K_{ex}

3: Calculate the concentration of each species [i] from the equation system at γ_i =1

4: Calculate γ_i from models using [i]

5: Calculate the concentration of each species [i]′ from the equation system

6: Calculation *F* parameter

$$OF = \frac{100}{Np} \Sigma \left(\left| \frac{\overline{[Zn]} - \overline{[Zn]}'}{\overline{[Zn]}} \right| + \left| \frac{\overline{[Ni]} - \overline{[Ni]}'}{\overline{[Ni]}} \right| \right)$$

7: If $OF > \varepsilon$

[i]=[i]′ and return to step 4

If $OF < \varepsilon$

$$OF = \frac{100}{Np} \left(\Sigma \left| \frac{\overline{[Zn]}^{Cal} - \overline{[Zn]}^{exp}}{\overline{[Zn]}^{exp}} \right| + \left| \frac{\overline{[Ni]}^{Cal} - \overline{[Ni]}^{exp}}{\overline{[Ni]}^{exp}} \right| \right)$$

8: If $OF > \varepsilon$

Calculate the concentration of each species [i]′ from the equation system and return to step 3

If $OF < \varepsilon$

Print parameters of models and K_x

---

3. 3. 1. Extraction Mechanism of Ni and Zn by D2EHPA

In this study, D2EHPA was used as a solvent extraction, which extracts Zn^{2+} and Ni^{2+}ions. The divalent extraction metals such as Ni^{2+} and Zn^{2+} using di-(2-ethylhexyl) phosphoric acid is shown using the equilibrium reaction (Equation (4)):

$$M_{(aq)}^{2+} + n\overline{(H_2A_2)}_{(org)} \leftrightarrow \overline{(MA_2(HA)_{2n-2})_{(org)}} + 2H_{(aq)}^{+} \quad (4)$$
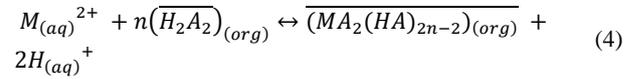
H_2A_2 is the extractant in dimeric form and the stoichiometric coefficient of H_2A_2 displayed by *n*. The D2EHPA molecules is well known being generally as dimers in the non-polar organic diluents. H_2A_2 shows the dimer of di-(2-ethylhexyl) phosphoric acid and the over -bar symbol illustrates the substances in the organic phase. K_{ex} parameter of the extraction reaction of Ni^{2+}, Zn^{2+} and D2EHPA can be given as Equation (5):

$$K_{ex} = \frac{\overline{[(MA_2(HA)_{2n-2})]}[H^+]^2}{[M^{2+}]\overline{[H_2A_2]}^n} \frac{\overline{\gamma}_{((MA_2(HA)_{2n-2}))} \cdot \gamma_{H^+}^2}{\gamma_{M^{2+}} \cdot \overline{\gamma}_{(H_2A_2)}^n} \quad (5)$$

and the distribution coefficient, *D*, can be expressed as Equation (6):

$$D = \frac{\overline{[(MA_2(HA)_{2n-2})]}}{[M^{2+}]} \quad (6)$$

By taking the logarithm of Equation (5) and by Equation (7):

$$log\, D - 2pH = nlog\left[\overline{(H_2A_2)}\right] + log\, K_{ex} - log \frac{\overline{\gamma}_{(MA_2(HA)_{2n-2})} \cdot \gamma_{H^+}^2}{\gamma_{M^{2+}} \cdot \overline{\gamma}_{(H_2A_2)}^n} \quad (7)$$

The equilibrium concentration of H_2A_2 in Equation (4) was considered by following (Equation (8)):

$$\left[\overline{(H_2A_2)}\right] = \left[\overline{(H_2A_2)}\right]^0 - n\,\overline{\left[(MA_2(HA)_{2n-2})\right]} \qquad (8)$$

The plot of $log\,D - pH$ *vs.* $log\left[\overline{(H_2A_2)}\right]$ is linear if the ideality is assumed for the system, i.e. $\gamma_i = 1$. The line slope (n) characterizes H_2A_2 stoichiometric coefficient whereas its intercept denotes K_{ex} without considering the non-ideality of the substances.

In ionic strength calculation, it is required to consider H^+, Na^+, NO^{-3}, Zn^{2+}, and Ni^{2+} ions in the aqueous solution. According to Equation (4), the metal ions during the extraction reaction are substituted with H^+. The organic solution contains of three components: Zn^{2+} and Ni^{2+}, free extractant dimers (H_2A_2), and kerosene as diluent. Therefore, the system contains five unknown concentrations and five equations were needed. The equations were obtained by charge and mass balances in the aqueous solution as following Equations (9-14):

$$[Kerosene\,] = [Kerosene]^0 \qquad (9)$$

$$[(H_2A_2)] = [(H_2A_2)]^0 - n\,[M^{2+}\,] \qquad (10)$$

$$[Na^+] = [M^{\,2+}]^0 \qquad (11)$$

$$[H^+] = [H^+]^\circ + [M^{\,2+}]^0 \qquad (12)$$

$$[Ni^{\,2+}] = [Ni^{2+}]^\circ - \overline{[Ni^{2+}]} \qquad (13)$$

$$[Zn^{\,2+}] = [Zn^{\,2+}]^\circ - \overline{[Zn^{2+}]} \qquad (14)$$

3. 3. 2. Determination of Stoichiometric Coefficient

The obtained experimental data that are used to obtained stoichiometric coefficient are shown in Table 1. The experimental tests were performed by D2EHPA (2-25 (v/v%)), at 298.15 K, 3.8 < pH < 4.5. In Equation (2), the slope analysis procedure is applied to calculate the organic complex of Zn^{2+} and Ni^{2+} and unknown n (stoichiometric coefficient) of D2EHPA dimer. Thus, the behavior of $log\,D - pH$ *vs.* $log(\overline{(H_2A_2)})$ must be plotted. Figure 5 demonstrates this behavior. Based on Figure 5, accuracy

TABLE 1. The extraction experimental data of zinc and nickel (O/A=1/1 and T = 298.15 K)

[Kerosene] (mol/L)	$[H_2A_2]^0$ (mol/L)	$[Ni]^0$ (mol/L)	$[Zn]^0$ (mol/L)	$\overline{[Ni]}$ (mol/L)	$\overline{[Zn]}$ (mol/L)	pH
4.175	0.025	0.0037	0.067	0.0002	0.0028	4.10
4.175	0.025	0.0037	0.067	0.0003	0.0028	4.15
4.067	0.050	0.0037	0.067	0.0005	0.0027	4.26
4.067	0.050	0.0037	0.067	0.0006	0.0039	4.10
4.019	0.075	0.0037	0.067	0.0007	0.0049	4.16
4.019	0.075	0.0037	0.067	0.0008	0.0073	4.20
4.067	0.050	0.0079	0.138	0.0017	0.0318	4.30
4.067	0.050	0.0079	0.138	0.0021	0.0987	4.10
4.067	0.050	0.0079	0.138	0.0018	0.1101	4.10
4.019	0.075	0.0079	0.138	0.0053	0.1269	3.99
4.019	0.075	0.0079	0.138	0.0093	0.1449	3.97
3.895	0.143	0.0079	0.138	0.0131	0.1591	4.10
3.895	0.143	0.0185	0.271	0.0154	0.1749	4.30
3.895	0.143	0.0185	0.271	0.0182	0.1914	4.32
3.690	0.287	0.0185	0.271	0.0252	0.2109	4.50
3.690	0.287	0.0185	0.271	0.0298	0.2564	4.31
3.690	0.287	0.0185	0.271	0.0356	0.3116	4.26
3.280	0.574	0.0438	0.469	0.0393	0.3378	4.18
3.280	0.574	0.0438	0.469	0.0397	0.3869	4.22
3.280	0.574	0.0438	0.469	0.0399	0.4125	4.13
3.280	0.574	0.0438	0.469	0.0432	0.4310	4.10
3.280	0.574	0.0438	0.469	0.0443	0.4364	4.11
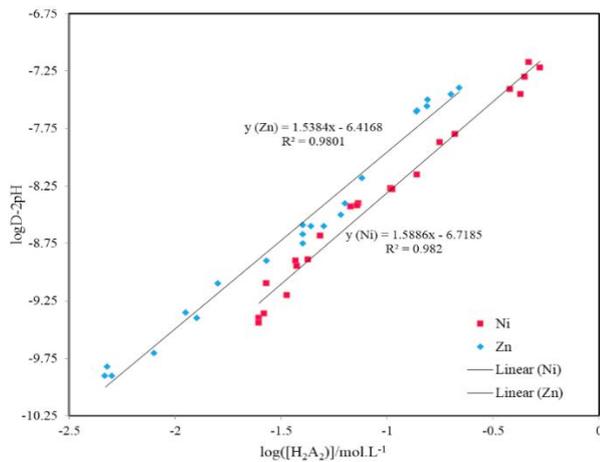
Figure 5. The *log (D-2pH)* behavior vs. *log([H2A2])*

of both correlations are satisfactory ($R^2 \geq 0.98$, R^2 is R-squared). According to curve fitting results, extraction reaction between D2EHPA, Zn^{2+} and Ni^{2+} dimers is as following Equation (15):

$$M^{2+} + 1.5(\overline{H_2A_2}) \leftrightarrow \overline{(MA_2(HA)} + 2H^+ \qquad (15)$$
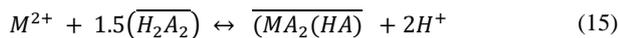
Using UNIQUAC-NRF, Electrolyte-UNIQUAC-NRF, NRTL and a new NRTL-based local composition model, the constant of Equation (15) was measured. All unknown parameters of four thermodynamic models are obtained based on experimental data. The obtained results were tabulated in Table 2. The unknown parameters were 17 and the details of them are as following: 12 unknown parameters of UNIQUAC-NRF and NRTL model and five unknown parameters of K_{ex} and Electrolyte-UNIQUAC-NRF and new NRTL-based local composition model. Furthermore, the values of q_i (surface parameter) and r_i (volume parameter), as structural parameters, of ionic and any molecular species were required in order to calculate γ_i coefficients. These coefficients are presented in literature [61].

To investigate the thermodynamic consistency of modeling of Zn^{2+} and Ni^{2+} extraction and to validate K_{ex} value and for calculation of the model factors, the obtained equilibrium concentration in the both phases were correlated with the experimental data. Consequently, the data that is given in Table 1 was classified in two parts. The first part of experimental data was related to find correctness of K_{ex} and factors of model, though the another part was compared to values predicted by these factors. Correctness of the calculations, in addition, was verified for both experimental data parts. According to Equation (4), the calculated values were achieved with adjusted correctness of K_{ex} values. γ_i were computed NRF by adjusted interaction factors and according to NRTL, new NRTL-based local composition model,

TABLE 2. The adjustable parameters based on all used models for zinc and nickel

Parameter		UNIQUAC-NRF	NRTL
I	j	α_{ij}	α_{ij}
Zn	Ni	5.64	4.90
Zn	HA	-6.43	-5.49
Zn	Kerosene	-2.02	-2.52
Ni	Zn	-4.51	-3.24
Ni	HA	6.16	5.12
Ni	Kerosene	1.15	1.58
HA	Zn	1.67	1.84
HA	Ni	-3.35	-3.56
HA	Kerosene	-0.27	-0.39
Kerosene	Zn	1.82	1.79
Kerosene	Ni	4.74	4.60
Kerosene	HA	-4.11	-4.28

		Electrolyte- UNIQUAC-NRF	New NRTL
		λ_{ij}	λ_{ij}
Zn^{2+}	NO_3^-	1.27	1.72
Ni^{2+}	NO_3^-	-4.65	-3.95
H^+	NO_3^-	-4.65	-4.28
Na^+	NO_3^-	3.10	3.67
Ion	Water	1.28	1.91

UNIQUAC-NRF and Electrolyte-UNIQUAC. Next, the values of equilibrium concentration were calculated by using the trust region dogleg iteration method. As can be shown in Figure 6, all obtained and calculated experimental data of Ni^{2+} and Zn^{2+} in the aqueous solution and organic media the at equilibrium condition.
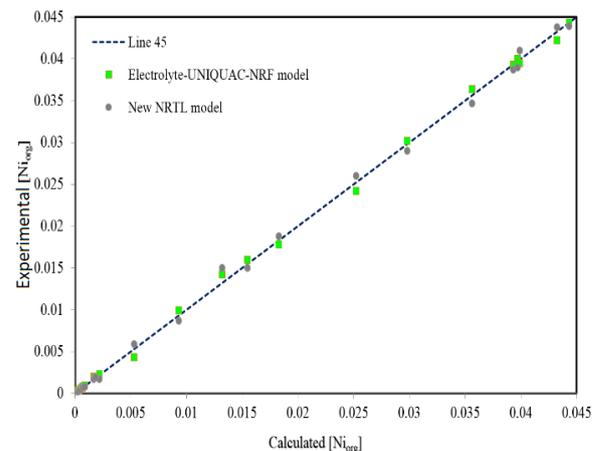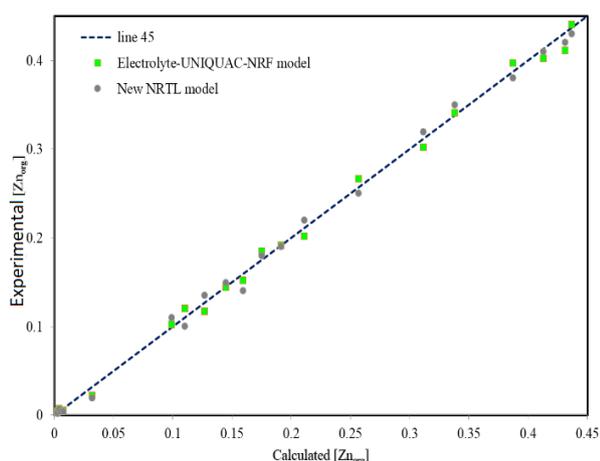
Figure 6. The Ni^{2+} and Zn^{2+} concentration in organic phase at 298.15 K: The experimental results vs. thermodynamic modeling.

4. CONCLUSIONS

This work was devoted to a comprehensive study of the extraction of Zn and Ni from zinc plant residue. The leaching behavior of metals in HNO_3 solution was investigated and the effect of some important parameter such as acid concentration, time, and temperature was studied. The result showed that increasing all these factors contributed to increase the leaching efficiency. About 100% of metal ions at the optimum extraction conditions: acid concentration of 2 M, temperature 358.15 K, S/L= 1/10, and 1.5 h was leached. The solvent extraction of Ni^{2+}, Zn^{2+}, and Pb^{2+} were examined from the leaching solution with D2EHPA. In one stage, the separation of Ni^{2+} and Zn^{2+} from Pb^{2+} was performed and about 99.8% of Ni^{2+} and Zn^{2+} were extracted (25 (v/v%) D2EHPA, pH = 5.5, (O/A) =1/1, and T = 298.15). Afterward, using various thermodynamic models, the concentration of organic and aqueous phases was simulated. The stoichiometry of the solvent extraction reaction was investigated by the slope analysis method, subsequently it was found that 1.5 D2EHPA molecules were required for the extraction of Ni^{2+} and Zn^{2+}. Therefore, the reaction was defined as $M^{2+} + 1.5 \left(\overline{H_2A_2} \right) \leftrightarrow \overline{(MA_2(HA)} + 2H^+$. Ni^{2+} and Zn^{2+} equilibrium concentrations were computed using a thermodynamic modeling. The γ_i for both organic and aqueous solutions were determined by UNIQUAC-NRF model, Electrolyte-UNIQUAC-NRF model, NRTL model and a new NRTL-based local composition model for electrolyte and non-electrolyte solution. The prediction of the equilibrium data of Ni^{2+} and Zn^{2+} by the calculated adjustable parameters demonstrated the accuracy of used thermodynamic models. As a result, Electrolyte-UNIQUAC-NRF and UNIQUAC-NRF equations in comparison the NRTL and a new local

based NRTL had more accuracy to calculate the extraction of Ni^{2+} and Zn^{2+} extraction by D2EHPA extractant from nitric solution and statistical processing of the results showed good consistency of experimental and calculated values.

5. REFERENCES

1. Kashyap, V. and Taylor, P., "Extraction and recovery of zinc and indium from residue rich in zinc ferrite", *Minerals Engineering*, Vol. 176, (2022), 107364. doi: 10.1016/j.mineng.2021.107364.

2. Kani, O.S.M., Azizitorghabeh, A. and Rashchi, F., "Recovery of zn (ii), mn (ii) and co (ii) from the zinc plant residue using the solvent extraction with cyanex 302 and d2ehpa/tbp: Stoichiometry and structural studies", *Minerals Engineering*, Vol. 169, (2021), 106944. doi: 10.1016/j.mineng.2021.106944.

3. Li, S., Yang, J., Wang, J., Han, B., Zhang, H., Yang, S. and Chen, Y., "Efficient zinc extraction with novel phenyl phosphate ptopp in sulfuric acid system", *Journal of Cleaner Production*, Vol. 417, (2023), 138052. doi: 10.1016/j.jclepro.2023.138052.

4. Asadollahzadeh, M., Shakib, B., Torab-Mostaedi, M. and Outokesh, M., "Extraction of molybdenum (vi) and vanadium (v) from nitrate solutions using coupling of acid and solvating extractants (research note)", *International Journal of Engineering, Transactions A: Basics*, Vol. 32, No. 10, (2019), 1366-1371. doi: 10.5829/IJE.2019.32.10A.05

5. Zhang, K., Qiu, L., Tao, J., Zhong, X., Lin, Z., Wang, R. and Liu, Z., "Recovery of gallium from leach solutions of zinc refinery residues by stepwise solvent extraction with n235 and cyanex 272", *Hydrometallurgy*, Vol. 205, (2021), 105722. doi: 10.1016/j.hydromet.2021.105722.

6. Liu, W., Li, J., Zheng, J., Song, Y., Shi, Z., Lin, Z. and Chai, L., "Different pathways for cr (iii) oxidation: Implications for cr (vi) reoccurrence in reduced chromite ore processing residue", *Environmental Science & Technology*, Vol. 54, No. 19, (2020), 11971-11979. doi: 10.1021/acs.est.0c01855

7. Igosawa, T., Matsumiya, M. and Sasaki, Y., "Recovery of tungsten compounds from spent tungstophosphate catalyst using leaching, solvent extraction with phosphonium-based ionic liquids and precipitation", *Hydrometallurgy*, Vol. 208, (2022), 105803. doi: 10.1016/j.hydromet.2021.105803.

8. Yuxin, Z., Ting, S., Hongyu, C., Ying, Z., Zhi, G., Suiyi, Z., Xinfeng, X., Hong, Z., Yidi, G. and Yang, H., "Stepwise recycling of fe, cu, zn and ni from real electroplating sludge via coupled acidic leaching and hydrothermal and extraction routes", *Environmental Research*, Vol. 216, (2023), 114462. doi: 10.1016/j.envres.2022.114462

9. Ahmadi, A., Sheibani, S., Mokmeli, M., Khorasani, S. and Yaghoobi, N., "Factors affecting the cathode edge nodulation in copper electrorefining process", *International Journal of Engineering, Transactions C: Aspects*, Vol. 35, No. 12, (2022), 2370-2376. doi: 10.5829/IJE.2022.35.12C.13.

10. Hosseinzadeh, M. and Alizadeh, M., "Improvement of the solvent extraction of rhenium from molybdenite roasting dust leaching solution using counter-current extraction by a mixer-settler extractor", *International Journal of Engineering, Transactions A: Basics*, Vol. 27, No. 4, (2014), 651-658. doi: 10.5829/idosi.ije.2014.27.04a.17.

11. Mohammadzadeh, M., Bagheri, H. and Ghader, S., "Study on extraction and separation of ni and zn using [bmim][pf6] il as selective extractant from nitric acid solution obtained from zinc plant residue leaching", *Arabian Journal of Chemistry*, Vol. 13, No. 6, (2020), 5821-5831. doi: 10.1016/j.arabjc.2020.04.019.

12. Suliman, S.S., Othman, N., Noah, N.F.M. and Kahar, I.N.S., "Extraction and enrichment of zinc from chloride media using emulsion liquid membrane: Emulsion stability and demulsification via heating-ultrasonic method", *Journal of Molecular Liquids*, Vol. 374, (2023), 121261. doi: 10.1016/j.molliq.2023.121261.

13. Asadollahzadeh, M., Torkaman, R. and Torab-Mostaedi, M., "Optimization of green technique develop for europium (iii) extraction by using phosphonium ionic liquid and central composite design approach", *International Journal of Engineering, Transactions B: Applications*, Vol. 34, No. 2, (2021), 508-516. doi: 10.5829/IJE.2021.34.02B.24.

14. Santanilla, A.J.M., Aliprandini, P., Benvenuti, J., Tenorio, J.A.S. and Espinosa, D.C.R., "Structure investigation for nickel and cobalt complexes formed during solvent extraction with the extractants cyanex 272, versatic 10 and their mixtures", *Minerals Engineering*, Vol. 160, (2021), 106691. doi: 10.1016/j.mineng.2020.106691.

15. Mahmoudi, A., Shakibania, S., Rezaee, S. and Mokmeli, M., "Effect of the chloride content of seawater on the copper solvent extraction using acorga m5774 and lix 984n extractants", *Separation and Purification Technology*, Vol. 251, (2020), 117394. doi: 10.1016/j.seppur.2020.117394.

16. Barnard, K.R., Zeng, L. and Shiers, D.W., "Stoichiometry of the nickel complex formed with lix 63 hydroxyoxime under acidic chloride conditions", *Solvent Extraction and Ion Exchange*, Vol. 40, No. 5, (2022), 477-492. doi: 10.1080/07366299.2021.1992891.

17. Odegbemi, F., Idowu, G.A. and Adebayo, A.O., "Nickel recovery from spent nickel-metal hydride batteries using lix-84i-impregnated activated charcoal", *Environmental Nanotechnology, Monitoring & Management*, Vol. 15, (2021), 100452. doi: 10.1016/j.enmm.2021.100452.

18. Valeev, D., Shoppert, A., Dogadkin, D., Romashova, T., Kuz'mina, T. and Salazar-Concha, C., "Extraction of al and rare earth elements via high-pressure leaching of boehmite-kaolinite bauxite using nh4hso4 and h2so4", *Hydrometallurgy*, Vol. 215, No., (2023), 105994. doi: 10.1016/j.hydromet.2022.105994.

19. Li, C., Jia, Y., Lu, X. and Chen, H., "Transport of zn (ii) through matrix enhanced polymer inclusion membrane containing oha and d2ehpa", *Chemical Engineering Journal*, Vol. 452, (2023), 139288. doi: 10.1016/j.cej.2022.139288.

20. Hou, H., Shao, S., Ma, B., Li, X., Shi, S., Chen, Y. and Wang, C., "Sustainable process for valuable-metal recovery from circulating fluidized bed fly ash through nitric acid pressure leaching", *Journal of Cleaner Production*, Vol. 360, (2022), 132212. doi: 10.1016/j.jclepro.2022.132212.

21. Martins, J.M.A., Guimaraes, A.S., Dutra, A.J.B. and Mansur, M.B., "Hydrometallurgical separation of zinc and copper from waste brass ashes using solvent extraction with d2ehpa", *Journal of Materials Research and Technology*, Vol. 9, No. 2, (2020), 2319-2330. doi: 10.1016/j.jmrt.2019.12.063.

22. Azizi, A., Nozhati, R.A. and Sillanpää, M., "Solvent extraction of copper and zinc from sulfate leach solution derived from a porcelain stone tailings sample with chemorex cp-150 and d2ehpa", *Journal of Sustainable Metallurgy*, Vol. 6, (2020), 250-258. doi: 10.1007/s40831-020-00271-w.

23. Hosseini, T., Mostoufi, N., Daneshpayeh, M. and Rashchi, F., "Modeling and optimization of synergistic effect of cyanex 302 and d2ehpa on separation of zinc and manganese", *Hydrometallurgy*, Vol. 105, No. 3-4, (2011), 277-283. doi: 10.1016/j.hydromet.2010.10.015

24. Babakhani, A., Rashchi, F., Zakeri, A. and Vahidi, E., "Selective separation of nickel and cadmium from sulfate solutions of spent nickel–cadmium batteries using mixtures of d2ehpa and cyanex 302", *Journal of Power Sources*, Vol. 247, (2014), 127-133. doi: 10.1016/j.jpowsour.2013.08.063.

25. Innocenzi, V. and Veglio, F., "Separation of manganese, zinc and nickel from leaching solution of nickel-metal hydride spent batteries by solvent extraction", *Hydrometallurgy*, Vol. 129, (2012), 50-58. doi: 10.1016/j.hydromet.2012.08.003.

26. Bagheri, H., Karimi, N., Dan, S., Notej, B. and Ghader, S., "Ionic liquid excess molar volume prediction: A conceptual comparison", *Journal of Molecular Liquids*, Vol. 336, (2021), 116581. doi: 10.1016/j.molliq.2021.116581.

27. Bagheri, H., Hashemipour, H., Ghalandari, V. and Ghader, S., "Numerical solution of particle size distribution equation: Rapid expansion of supercritical solution (ress) process", *Particuology*, Vol. 57, (2021), 201-213. doi: 10.1016/j.partic.2020.12.011.

28. Mokhtari, A., Bagheri, H., Ghazvini, M. and Ghader, S., "New mathematical modeling of temperature-based properties of ionic liquids mixture: Comparison between semi-empirical equation and equation of state", *Chemical Engineering Research and Design*, Vol. 177, (2022), 331-353. doi: 10.1016/j.cherd.2021.10.039.

29. Maraki, M., Tagimalek, H., Azargoman, M., Khatami, H. and Mahmoodi, M., "Experimental investigation and statistical modeling of the effective parameters in charpy impact test on az31 magnesium alloy with v-shape groove using taguchi method", *International Journal of Engineering, Transactions C: ASpects,*, Vol. 33, No. 12, (2020), 2521-2529. doi: 10.5829/IJE.2020.33.12C.13.

30. Iloeje, C.O., Jové Colón, C.F., Cresko, J. and Graziano, D.J., "Gibbs energy minimization model for solvent extraction with application to rare-earths recovery", *Environmental Science & Technology*, Vol. 53, No. 13, (2019), 7736-7745. doi: 10.1021/acs.est.9b01718

31. Razavi, S.M., Haghtalab, A. and Khanchi, A.R., "Thermodynamic modeling of the solvent extraction equilibrium for the recovery of vanadium (v) from acidic sulfate solutions using di-(2-ethylhexyl) phosphoric acid", *Fluid Phase Equilibria*, Vol. 474, (2018), 20-31. doi: 10.1016/j.fluid.2018.07.007.

32. Razavi, S.M., "A new nrtl-based local composition model for thermodynamic modeling of electrolyte solutions", *The Journal of Chemical Thermodynamics*, Vol. 161, (2021), 106534. doi: 10.1016/j.jct.2021.106534.

33. Liu, F., Ning, P.-G., Cao, H.-B. and Zhang, Y., "Measurement and modeling for vanadium extraction from the (navo3+ h2so4+ h2o) system by primary amine n1923", *The Journal of Chemical Thermodynamics*, Vol. 80, (2015), 13-21. doi: 10.1016/j.jct.2021.106534.

34. Aman-Pommier, F. and Jallut, C., "Solubility of diazepam in water+ tert-butyl alcohol solvent mixtures: Part 2. Correlation using scatchard-hildebrand and combined scatchard-hildebrand/flory-huggins excess gibbs energy models", *Fluid Phase Equilibria*, Vol. 458, (2018), 84-101. doi: 10.1016/j.jct.2021.106534.

35. Mörters, M. and Bart, H.-J., "Extraction equilibria of zinc with bis (2-ethylhexyl) phosphoric acid", *Journal of Chemical & Engineering Data*, Vol. 45, No. 1, (2000), 82-85. doi: 10.1021/je990200u.

36. Shi, D., Cui, B., Li, L., Xu, M., Zhang, Y., Peng, X., Zhang, L., Song, F. and Ji, L., "Removal of calcium and magnesium from lithium concentrated solution by solvent extraction method using d2ehpa", *Desalination*, Vol. 479, (2020), 114306. doi: 10.1016/j.desal.2019.114306.

37. Tanong, K., Tran, L.-H., Mercier, G. and Blais, J.-F., "Recovery of zn (ii), mn (ii), cd (ii) and ni (ii) from the unsorted spent batteries using solvent extraction, electrodeposition and

precipitation methods", *Journal of Cleaner Production*, Vol. 148, (2017), 233-244. doi: 10.1016/j.jclepro.2017.01.158.

38. Babakhani, A. and Sartaj, M., "Removal of cadmium (ii) from aqueous solution using tripolyphosphate cross-linked chitosan", *Journal of Environmental Chemical Engineering*, Vol. 8, No. 4, (2020), 103842. doi: 10.1016/j.jece.2020.103842.

39. Pitzer, K.S. and Silvester, L.F., "Thermodynamics of electrolytes. Vi. Weak electrolytes including h 3 po 4", *Journal of Solution Chemistry*, Vol. 5, (1976), 269-278. doi: 10.1016/j.jece.2020.103842.

40. Pitzer, K.S. and Mayorga, G., "Thermodynamics of electrolytes. Ii. Activity and osmotic coefficients for strong electrolytes with one or both ions univalent", *The Journal of Physical Chemistry*, Vol. 77, No. 19, (1973), 2300-2308. doi: 10.1021/j100638a009.

41. Pitzer, K.S., "Activity coefficients in electrolyte solutions, CRC press, (2018).

42. Pitzer, K.S., "Thermodynamics of electrolytes. I. Theoretical basis and general equations", *The Journal of Physical Chemistry*, Vol. 77, No. 2, (1973), 268-277. doi: 10.1021/j100621a026.

43. Cruz, J.L. and Renon, H., "A new thermodynamic representation of binary electrolyte solutions nonideality in the whole range of concentrations", *AIChE Journal*, Vol. 24, No. 5, (1978), 817-830. doi: 10.1002/aic.690240508.

44. Zhao, E., Yu, M., Sauvé, R.E. and Khoshkbarchi, M.K., "Extension of the wilson model to electrolyte solutions", *Fluid Phase Equilibria*, Vol. 173, No. 2, (2000), 161-175. doi: 10.1016/S0378-3812(00)00393-9.

45. Thomsen, K., Rasmussen, P. and Gani, R., "Correlation and prediction of thermal properties and phase behaviour for a class of aqueous electrolyte systems", *Chemical Engineering Science*, Vol. 51, No. 14, (1996), 3675-3683. doi: 10.1016/0009-2509(95)00418-1.

46. Chen, C.C. and Evans, L.B., "A local composition model for the excess gibbs energy of aqueous electrolyte systems", *AIChE Journal*, Vol. 32, No. 3, (1986), 444-454. doi: 10.1208/s12249-019-1373-4.

47. Haghtalab, A. and Vera, J., "A nonrandom factor model for the excess gibbs energy of electrolyte solutions", *AIChE Journal*, Vol. 34, No. 5, (1988), 803-813. doi: 10.1002/aic.690340510.

48. Sadeghi, R., "New local composition model for electrolyte solutions", *Fluid Phase Equilibria*, Vol. 231, No. 1, (2005), 53-60. doi: 10.1016/j.molliq.2011.10.015.

49. Chen, C.-C. and Mathias, P.M., "Applied thermodynamics for process modeling", *American Institute of Chemical Engineers. AIChE Journal*, Vol. 48, No. 2, (2002), 194. doi: 10.1002/aic.690480202.

50. Renon, H. and Prausnitz, J.M., "Local compositions in thermodynamic excess functions for liquid mixtures", *AIChE Journal*, Vol. 14, No. 1, (1968), 135-144. doi: 10.1002/aic.690140124.

51. Haghtalab, A. and Peyvandi, K., "Generalized electrolyte-uniquac-nrf model for calculation of solubility and vapor pressure of multicomponent electrolytes solutions", *Journal of Molecular Liquids*, Vol. 165, No., (2012), 101-112. doi: 10.1016/j.molliq.2011.10.015.

52. Mohammadzadeh, M., Bagheri, H. and Ghader, S., "Solvent extraction of nickel and zinc from nitric acid solution using d2ehpa: Experimental and modeling", *Journal of Solution Chemistry*, Vol. 51, No. 4, (2022), 424-447. doi: 10.1007/s10953-022-01151-5.

53. Sethurajan, M., Huguenot, D., Jain, R., Lens, P.N., Horn, H.A., Figueiredo, L.H. and van Hullebusch, E.D., "Leaching and selective zinc recovery from acidic leachates of zinc

metallurgical leach residues", *Journal of Hazardous Materials*, Vol. 324, (2017), 71-82. doi: 10.1016/j.jhazmat.2021.125664.

54. Safarzadeh, M.S., Moradkhani, D., Ilkhchi, M.O. and Golshan, N.H., "Determination of the optimum conditions for the leaching of cd–ni residues from electrolytic zinc plant using statistical design of experiments", *Separation and Purification Technology*, Vol. 58, No. 3, (2008), 367-376. doi: 10.1016/j.seppur.2007.05.016.

55. Randhawa, N.S., Gharami, K. and Kumar, M., "Leaching kinetics of spent nickel–cadmium battery in sulphuric acid", *Hydrometallurgy*, Vol. 165, (2016), 191-198. doi: 10.1016/j.hydromet.2015.09.011.

56. Aghazadeh, S., Gharabaghi, M. and Shafaei, Z., "Thermodynamical and catalytic aspects of zinc separation from aqueous solution", *Chinese Journal of Chemical Engineering*, Vol. 26, No. 12, (2018), 2455-2460. doi: 10.1016/j.cjche.2018.07.022.

57. Aghdam, A.A.B., Yoozbashizadeh, H. and Moghaddam, J., "Simple separation method of zn (ii) and cd (ii) from brine solution of zinc plant residue and synthetic chloride media using solvent extraction", *Chinese Journal of Chemical Engineering*, Vol. 28, No. 4, (2020), 1055-1061. doi: 10.1016/j.cjche.2019.12.003.

58. Sheik, A., Ghosh, M., Sanjay, K., Subbaiah, T. and Mishra, B., "Dissolution kinetics of nickel from spent catalyst in nitric acid medium", *Journal of the Taiwan Institute of Chemical Engineers*, Vol. 44, No. 1, (2013), 34-39. doi: 10.1016/j.jtice.2012.08.003.

59. Assefi, M., Maroufi, S., Mayyas, M. and Sahajwalla, V., "Recycling of ni-cd batteries by selective isolation and hydrothermal synthesis of porous nio nanocuboid", *Journal of Environmental Chemical Engineering*, Vol. 6, No. 4, (2018), 4671-4675. doi: 10.1016/j.jece.2018.07.021.

60. Yu, S., Xing, W., Xue, F., Cheng, Y. and Li, B., "Solubility and thermodynamic properties of nimodipine in pure and binary solvents at a series of temperatures", *The Journal of Chemical Thermodynamics*, Vol. 152, (2021), 106259. doi: 10.1016/j.jct.2020.106259.

61. Ravichandran, A., Khare, R. and Chen, C.C., "Predicting nrtl binary interaction parameters from molecular simulations", *AIChE Journal*, Vol. 64, No. 7, (2018), 2758-2769. doi: 10.1002/aic.16117.

62. Pinto, I.S. and Soares, H.M., "Selective leaching of molybdenum from spent hydrodesulphurisation catalysts using ultrasound and microwave methods", *Hydrometallurgy*, Vol. 129, (2012), 19-25. doi: 10.1016/j.hydromet.2012.08.008.

63. Spooren, J., Binnemans, K., Björkmalm, J., Breemersch, K., Dams, Y., Folens, K., González-Moya, M., Horckmans, L., Komnitsas, K. and Kurylak, W., "Near-zero-waste processing of low-grade, complex primary ores and secondary raw materials in europe: Technology development trends", *Resources, Conservation and Recycling*, Vol. 160, (2020), 104919. doi: 10.1016/j.resconrec.2020.104919.

64. Haghtalab, A. and Peyvandi, K., "Electrolyte-uniquac-nrf model for the correlation of the mean activity coefficient of electrolyte solutions", *Fluid Phase Equilibria*, Vol. 281, No. 2, (2009), 163-171. doi: 10.1016/j.fluid.2009.04.013.

65. Asamoah, R.K., Skinner, W. and Addai-Mensah, J., "Alkaline cyanide leaching of refractory gold flotation concentrates and bio-oxidised products: The effect of process variables", *Hydrometallurgy*, Vol. 179, (2018), 79-93. doi: 10.1016/j.hydromet.2018.05.010.

66. Shen, X., Shao, H., Liu, Y. and Zhai, Y., "Extraction, phase transformation and kinetics of valuable metals from nickel-chromium mixed metal oxidized ore", *Minerals Engineering*, Vol. 161, (2021), 106737. doi: 10.1016/j.mineng.2020.106737.

6. Appendix A

6. 1. UNIQUAC-NRF Model

In order to correlate the activity coefficient for aqueous nonelectrolyte systems the UNIQUAC-NRF model is investigated [32, 51]. This model consists of two terms as a combinatorial for entropic contribution, and a residual for enthalpy contribution. Therefore, the activity coefficient equations for each component in a multicomponent mixture are given as following:

$$Ln\,\gamma_i = Ln\,\gamma_i^c - Ln\,\gamma_i^r \tag{A.1}$$

$$Ln\,\gamma_i^c = Ln\left(\frac{\Phi_i}{x_i}\right) + 1 - \left(\frac{\Phi_i}{x_i}\right) - \frac{z}{2}q_i\left[Ln\left(\frac{\Phi_i}{\theta_i}\right) + 1 - \left(\frac{\Phi_i}{\theta_i}\right)\right] \tag{A.2}$$

$$Ln\,\gamma_i^r = q_i\left[1 + Ln\,\Gamma_{ii}\;\sum_{j=1}^n(\theta_j\,\Gamma_{ij}) + \right.$$
$$(1-\theta_i)\sum_{\substack{j=1\\j\neq i}}^n\left(\theta_j\,Ln\,\frac{\Gamma_{ij}\Gamma_{ji}}{\Gamma_{ii}\Gamma_{jj}}\right) -$$
$$\left.\frac{1}{2}\sum_{\substack{k=1\\k\neq i}}^n\sum_{\substack{l=1\\l\neq i,\,k}}^n\left(\theta_k\theta_l\,Ln\,\frac{\Gamma_{kl}\Gamma_{lk}}{\Gamma_{kk}\Gamma_{ll}}\right)\right] \tag{A.3}$$

where Z is the coordination number, x_i denotes mole fraction of each component. The volume fraction (ϕ_i) and area fraction (θ_i) of each species are defined as following:

$$\theta_i = \frac{x_i q_i}{\sum_j x_j q_j} \tag{A.4}$$

$$\Phi_i = \frac{x_i r_i}{\sum_j x_j r_j} \tag{A.5}$$

The nonrandom factor, Γ_{ij}, is defined as following:

$$\Gamma_{ij} = \frac{\tau_{ij}}{\sum_k \theta_k \tau_{kj}} \tag{A.6}$$

where τ_{ij} and τ_{ji} are the interaction parameters of UNIQUAC-NRF model for i and j components that are related to the interaction energies (u_{ij}) as following:

$$\tau_{ij} = exp\left(-\frac{(u_{ij}-u_{jj})}{RT}\right) = exp(-\alpha_{ij}) \tag{A.7}$$

$$\alpha_{ij} = (\alpha_{ij})_0 + (\alpha_{ij})_0\left(\frac{1}{T}-\frac{1}{298.15}\right) + (\alpha_{ij})_2\left(\frac{298.15-T}{T}+Ln\frac{T}{298.15}\right) \tag{A.8}$$

where x_i is mole fraction, Z is coordination number, τ_{ij} and τ_{ji} are the interaction factors.

6. 2. Electrolyte-UNIQUAC-NRF Model

The Electrolyte-UNIQUAC-NRF model is based on the local composition approach for the calculation of activity coefficients in electrolyte solutions. Here the main equations of the model were provided. This activity coefficient model consists of a long range interaction contribution represented by the Pitzer-Debye-Hückel equation, and a short range interaction contribution which itself is stated as the sum of a combinatorial term and a residual term as following [62]:

$$Ln\,\gamma_i = (Ln\,\gamma_i^*)^{PDH} + (Ln\,\gamma_i^*)^c + (Ln\,\gamma_i^*)^r \tag{A.9}$$

where star superscript stands for unsymmetrical normalization.

$$(Ln\,\gamma_i^*)^{PDH} = -A_\emptyset\left(\frac{1000}{M_S}\right)^{0.5}\left[\left(\frac{2z_e^2}{\rho}\right)Ln\,(1+\rho I_x^{0.5}) + \frac{z_e^2 I_x^{0.5}-2I_x^{1.5}}{1+\rho I_x^{0.5}}\right] \tag{A.10}$$

where M_S is the molecular weight of solvent, z is the charge number of each ion, ρ is closest approach parameter, A_ϕ is the Debye-Hückel constant, and I_x stands for the ionic strength on a mole fraction basis.

$$(Ln\,\gamma_i^*)^c = (Ln\,\gamma_i)^c - (Ln\,\gamma_i^\infty)^c \tag{A.11}$$

$$(Ln\,\gamma_i)^c = Ln\left(\frac{\Phi_i'}{X_i}\right) + 1 - \left(\frac{\Phi_i'}{X_i}\right) - \frac{z}{2}q_i\left[Ln\left(\frac{\Phi_i'}{\theta_i'}\right) + 1 - \left(\frac{\Phi_i'}{\theta_i'}\right)\right] \tag{A.12}$$

$$(Ln\,\gamma_i^\infty)^c = Ln\left(\frac{r_i}{r_s}\right) - \frac{z}{2}q_i\left[Ln\left(\frac{r_i q_s}{r_s q_i}\right) - \left(\frac{r_i q_s}{r_s q_i}\right) + 1\right] - \left(\frac{r_i}{r_s}\right) + 1 \tag{A.13}$$

where Z is coordination number, and r_i and q_i denote the volume and surface parameters of ion i or solvent molecules. The effective volume and area fractions of each species are expressed as following:

$$\Phi_i' = \frac{X_i r_i}{\sum_j X_j r_j} \tag{A.14}$$

$$\theta_i' = \frac{X_i q_i}{\sum_j X_j q_j} \tag{A.15}$$

where X stands for the effective mole fraction that is expressed by the bulk mole fraction as $X_i = C_i x_i$, in which $C_i = z_i$ for ions and $C_i = 1$ for solvent molecules. Finally, the residual term of activity coefficient as following:

$$(Ln\,\gamma_i^*)^r = (Ln\,\gamma_i)^r - (Ln\,\gamma_i^\infty)^r \tag{A.16}$$

$$\frac{1}{q_a z_a}(Ln\,\gamma_a)^r = \sum_{a'}\frac{\theta_{a'}'}{z_{a'}}\left(1 - \sum_{c'}\theta_{c'}'\,Ln\,(\tau_{c'a'})\right) + \sum_{c'}\frac{\theta_{c'}'}{z_{c'}}\left(1 - \Gamma_{ac'} + Ln\,(\tau_{ac'}) - \sum_{a'}\theta_{a'}'\,Ln\,(\tau_{c'a'})\right) + \theta_m'\left(1 - \Gamma_{am} + Ln\,(\tau_{am}) - \sum_i\theta_i'\,Ln\,(\tau_{im})\right) - \frac{1}{z_a}\left(Ln\left(\sum_{c'}\theta_{c'}'\,\tau_{c'a} + \theta_m'\right) - \sum_{c'}\theta_{c'}'\,Ln\,(\tau_{c'a})\right) \tag{A.17}$$

$$\frac{1}{q_c z_c}(Ln\,\gamma_c)^r = \sum_{c'}\frac{\theta_{c'}'}{z_{c'}}\left(1 - \sum_{a'}\theta_{a'}'\,Ln\,(\tau_{a'c'})\right) + \sum_{a'}\frac{\theta_{a'}'}{z_{a'}}\left(1 - \Gamma_{ca'} + Ln\,(\tau_{ca'}) - \sum_{c'}\theta_{c'}'\,Ln\,(\tau_{c'a'})\right) + \theta_m'\left(1 - \Gamma_{cm} + Ln\,(\tau_{cm}) - \sum_i\theta_i'\,Ln\,(\tau_{im})\right) - \frac{1}{z_c}\left(Ln\left(\sum_{a'}\theta_{a'}'\,\tau_{a'c} + \theta_m'\right) - \sum_{a'}\theta_{a'}'\,Ln\,(\tau_{a'c})\right) \tag{A.18}$$

$$(Ln\,\gamma_i^\infty)^r = q_i z_i\,(1 - \tau_{im} + Ln\,\tau_{im}) \tag{A.19}$$

where c, a, and m subscripts show the cations, anions, and solvent molecules, respectively. The ion-molecule and ion-ion interaction energy parameters are represented by τ. The interaction energy parameters of the model are written as following:

$$\tau_{am} = \tau_{am} = exp(-\lambda_{ion,m}) \tag{A.20}$$

$$\tau_{ac} = \tau_{ac} = exp(-\lambda_{c,a}) \tag{A.21}$$

$$\lambda_{ij} = (\lambda_{ij})_0 + (\lambda_{ij})_0 \left(\frac{1}{T} = \frac{1}{298.15}\right) + (\lambda_{ij})_2 \left(\frac{298.15-T}{T} + Ln\,\frac{T}{298.15}\right) \tag{A.22}$$

where $\lambda_{ion,m}$ and $\lambda_{c,a}$ are the adjustable parameters of the model.

6. 3. NRTL Model   The NRTL model is following [59]:

$$\frac{g^M}{RT} = \sum_{i=1}^n x_i\,Ln(x_i) + \frac{g^E}{RT} \tag{A.23}$$

$$\frac{g^E}{RT} = \sum_{i=1}^n x_i\,\frac{\sum_{i=1}^n \tau_{ji} G_{ji} x_j}{\sum_{i=1}^n G_{Ki}\,x_k} \tag{A.24}$$

$$G_{ij} = exp\,(-\alpha_{ij}\,\tau_{ij}) \tag{A.25}$$

$$\tau_{ij} = \frac{g_{ij} - g_{jj}}{RT} = \frac{\Delta g_{ij}}{RT} \tag{A.26}$$

Here, g_{ij} is an energy factor that illustrates the interaction of species i and j, and the factor R_{ij}, R_{ji} is correlated to the non-randomness in the mixture (R_{ij}) corresponds to complete randomness, or an ideal solution.

6. 4. New NRTL-based Local Composition Model
The new NRTL model is given as following [61]:

$$g_c = Z_c(\sum_{a'} X_{a'c}\,g_{a'c} + \sum_{m'} X_{m'c}\,g_{m'c}) \tag{A.27}$$

$$g_a = Z_a(\sum_{c'} X_{c'a}\,g_{c'a} + \sum_{m'} X_{m'a}\,g_{m'a}) \tag{A.28}$$

$$g_m = \sum_i X_{im}\,g_{im} \tag{A.29}$$

where the g_c (cation Gibbs energy), g_a (anion energy) and g_m (solvent Gibbs energy) are as following [59, 61]:

$$g_c^{ref} = Z_c \left(\frac{\sum_{a'} X_{a'} g_{a'c} + \sum_{m'} X_{m'} g_{m'c}}{\sum_{a'} X_{a'} + \sum_{m'} X_{m'}}\right) \tag{A.30}$$

$$g_a^{ref} = Z_a \left(\frac{\sum_{c'} X_{c'} g_{c'a} + \sum_{m'} X_{m'} g_{m'a}}{\sum_{c'} X_{c'} + \sum_{m'} X_{m'}}\right) \tag{A.31}$$

$$g_m^{ref} = \frac{\sum_i X_{im} g_{im}}{\sum_i X_i} \tag{A.32}$$

The excess molar Gibbs energy function is obtained as following [61]:

$$\frac{(g^E)_{SR}}{RT} =$$
$$\sum_{a'} X_{a'} \left[\sum_{j \neq a} \frac{X_i}{\sum_{j \neq a} X_j} \left(\frac{\sum_{k \neq a} X_k G_{ka',ia'} \tau_{ka',ia'}}{\sum_{k \neq a} X_k G_{ka',ia'}}\right)\right] +$$
$$\sum_{c'} X_{c'} \left[\sum_{i \neq c} \frac{X_i}{\sum_{i \neq c} X_j} \left(\frac{\sum_{i \neq c} X_k G_{kc',ic'} \tau_{kc',ic'}}{\sum_{k \neq c} X_k G_{kc',ic'}}\right)\right] +$$
$$\sum_{m'} X_{m'} \left[\left(\frac{\sum_k X_k G_{km',m'm'} \tau_{km',m'm'}}{\sum_k X_k G_{km',m'm'}}\right) - \left(\sum_k X_k\,\tau_{km',m'm'}\right)\right] \tag{A.33}$$

And activity coefficients are given as following [61]:

$$Ln\gamma_i = \frac{\partial\left(n_t \frac{g^E}{RT}\right)}{\partial n_i} \tag{A.34}$$

$$Ln\gamma_i = (Ln\gamma_i^*)_{LR} + (Ln\gamma_i^*)_{SR} \tag{A.35}$$

$$(Ln\gamma_i^*)_{LR} = -A_\emptyset \left(\frac{1000}{M_S}\right)^{0.5} \left[\left(\frac{2z_e^2}{\rho}\right) Ln\,(1 + \rho I_x^{0.5}) + \frac{z_e^2 I_x^{0.5} - 2I_x^{1.5}}{1 + \rho I_x^{0.5}}\right] \tag{A.36}$$

$$(Ln\gamma_i^*)_{LR} = -A_\emptyset \left(\frac{1000}{M_S}\right)^{0.5} \frac{2I_x^{1.5}}{1 + \rho I_x^{0.5}} \tag{A.37}$$

$$(Ln\gamma_i^*)_{SR} = (Ln\gamma_i)_{SR} + (Ln\gamma_i^\infty)_{SR} \tag{A.38}$$

$$(Ln\gamma_i^\infty)_{SR} = Z_i(G_{im,mm} - 1)\,\tau_{im,mm} \tag{A.39}$$

$$\tau_{ij,kj} = (\lambda_{ij})_0 + (\lambda_{ij})_0 \left(\frac{1}{T} = \frac{1}{298.15}\right) + (\lambda_{ij})_2 \left(\frac{298.15-T}{T} + Ln\,\frac{T}{298.15}\right) \tag{A.40}$$

Persian Abstract

چکیده

پسماند فیلترکیک روی حاوی فلزات ارزشمندی است که می توان از آنها به عنوان منبعی برای به دست آوردن این فلزات استفاده مجدد کرد. این مطالعه یک مطالعه تجربی دو مرحله ای استخراج روی و نیکل از فیلترکیک روی را توصیف می‌کند که شامل لیچینگ فیلترکیک روی و سپس استخراج فلزات به کمک فاز آلی از محلول لیچینگ است. برای تعیین شرایط بهینه لیچینگ، یک مطالعه جامع از بازیابی عناصر شیمیایی از فیلتر کیک مصرف شده به صورت تجربی در سطوح مختلف غلظت اسید در دماهای مختلف در حالی که غلظت عناصر شیمیایی با زمان اندازه‌گیری شد، مورد مطالعه قرار گرفت. نتایج تجربی نشان داد که۹۹ درصدازنیکل و روی و ۸۹ درصد از سرب در شرایط بهینه دومولار نیتریک اسید، زمان t=1.5h، دمای   T= 358.15 K، نسبت فاز و S/L=1. / 10قابل دستیابی هستند. سپس استخراج نیکل،روی و سرب توسط استخراج کننده دی-(۲- اتیل هگزیل) فسفریک اسید(D2EHPA) به همراه رقیق کننده کروزن بررسی گردید. pHو غلظت استخراج کننده به عنوان متغیرهای موثر بر استخراج در نظر گرفته شدند. نتایج نشان داد افزایش pHو غلظت استخراج کننده تاثیر چشم گیری در استخراج نیکل و روی دارد و در شرایط بهینه pH = 5.5، D2EHPA (v/v%) ۲۵و (O/A) = ۹۵،1/1 و ۹۰ درصد از روی و نیکل استخراج شدند. برای مدل‌سازی غلظت‌های تعادل در فازهای آلی و آبی و محاسبه ضرایب فعالیت، از مدل‌های ترکیب موضعی مبتنی بر Electrolyte-UNIQUAC-NRF، UNIQUAC-NRF، NRTL و NRTL-based local composition models استفاده شد. پس از آن، پارامترهای تنظیم شده با موفقیت برای محاسبه ثابت تعادل پارامترهای مجهول و واکنش استخراج استفاده شد. نتایج به‌دست‌آمده از مدل‌سازی ترمودینامیکی با داده‌های تجربی مطابقت خوبی داشت.